Karlsruher Institut für Technologie
Institut für Baustatik

Composite Repair of Through-Wall Defects in Pipework - Analytical and Numerical Models with respect to ISO/TS 24817

M. Köpple, S. Lauterbach, W. Wagner

Mitteilung 2(2012)

BAUSTATIK

Karlsruher Institut für Technologie
Institut für Baustatik

Composite Repair of Through-Wall Defects in Pipework - Analytical and Numerical Models with respect to ISO/TS 24817

M. Köpple, S. Lauterbach, W. Wagner

Mitteilung 2(2012)

© Prof. Dr.–Ing. W. Wagner
Institut für Baustatik
Karlsruher Institut für Technologie
Kaiserstr. 12
76131 Karlsruhe

Telefon: +49 721 608 42280
Telefax: +49 721 608 46015
E–mail: info@ibs.kit.edu
Internet: http://www.ibs.kit.edu

Composite Repair of Through-Wall Defects in Pipework - Analytical and Numerical Models with respect to ISO/TS 24817

M.F. Köpple, S. Lauterbach, W. Wagner

Karlsruhe Institute of Technology (KIT), Institute for Structural Analysis, Kaiserstr. 12, 76131 Karlsruhe, Germany

Abstract

A major problem for the oil and gas industry is the repair of corroded steel piping. As a replacement of affected sections usually results in high expenses for the operator, rehabilitation methods which can be implemented on an operating pipeline are favoured by the industry. The application of overwraps made of Fibre-Reinforced Polymer systems offers such a promising method. In this work it is assumed that an overwrap is already installed, however, ongoing internal corrosion leads to a through-wall defect in the pipe. Hence, the fluid pressurises the repair and a detachment of the overwrap from the steel substrate can occur. This can even result in external leakage. In order to avoid this case of damage an analytical assessment approach is developed by means of Linear Elastic Fracture Mechanics and Finite Element Analysis. Subsequently, this approach is compared to the one given in the Code ISO/TS 24817 which is currently the mainly used code for the qualification and design of composite repairs for pipework.

Keywords: Pipeline corrosion, FRP overwrap, Plate theory, Fracture mechanics, Finite element analysis (FEA)

1. Introduction

The oil and gas industry uses steel pipelines as a basic element in the production and transport of oil and gas. Operating in harsh environmental conditions and transporting a wide range of high-pressure fluids, pipelines can suffer from a variety of damage scenarios. These may include coating damage, erosion, corrosion or mechanical damage. One of the most common scenarios experienced by the industry is internal and/or external corrosion of the piping. Depending on the severity of the problem this can have significant detrimental effects on the pressure bearing capability of the pipelines and may lead to reduced life spans or at worst to a loss of structural integrity, i.e. failure. In order to extend the durability of pipelines, methods to repair such damage have been developed.

A repair must be able to prevent leakage and also to restore all or part of the maximum allowable operating capacity of the pipeline. Usually, traditional repair methods require that the corroded or damaged piping is taken offline while the affected pipe section is replaced or reinforced by external steel strengthening/sealing elements. However, a plant shutdown imposes a significant loss in revenue on the operator. Consequently, rehabilitation methods which can be implemented without shutting down the production are favoured by the industry [1].

The use of *Fibre-Reinforced Polymer* (FRP) systems for rehabilitation and retrofitting of deteriorating structural systems has been embraced worldwide. FRP materials are highly suited for use as repair material as they possess a very high specific strength and stiffness, a high formability and an inherent immunity to corrosion [2]. Hence, they have emerged in many industries over the past decades including aerospace, automotive, infrastructure and oil and gas. In the concrete and bridge industry, for instance, the load-carrying capacity of reinforced concrete beams can be improved significantly by bonding FRP laminates to its tension flange [3, 4]. A recent application of FRPs for the oil and gas industry involves the repair of corroded pipelines by external wrapping of affected sections. Primary benefits associated with FRP overwrap repairs are a continuous fluid transmission while the repair is installed and the fact that no hot work or ignition is required and thus, the explosion potential is eliminated. This results in a significant improvement and reduction in repair costs [5, 6].

A major disadvantage in the use of FRP repairs is the complexity of possible failure mechanisms which can range from intra-laminar failure (e.g. fibre fracture or fibre-matrix debonding) to inter-laminar failure, also known as delamination [7, 8]. If delamination occurs between two different materials, it is called bi-material interface fracture.

In this paper fracture between a steel pipeline and an applied overwrap made of FRP is discussed. Therefore, it is assumed that ongoing internal corrosion leads to a relatively uniform loss of metal thickness and in extreme case to a through-wall defect in the pipeline. As a result the internal fluid pressure of the operating pipeline acts on the FRP/steel interface and a pressurised blister in the repair occurs. If the detachment of the repair from the pipeline propagates it results in external leakage. In order to ensure the applicability of FRP overwrap repair systems in case of internal corrosion, the processes of burst and leakage have to be investigated in detail. Previous work done by Mableson et al. [9] has shown that tubular pipe test samples and representative flat plate test samples, both composed of a steel substrate and a FRP repair, where blind holes were drilled into the steel, fail at very similar pressures. As a consequence, it is assumed that the effects of wall curvature can be neglected compared to the local stresses involved in the blister. And hence, flat plate models are regarded as a first approximation model to investigate delamination and blistering of an FRP overwrap repair system, respectively to deduce an analytical assessment approach which can be applied by the industry.
This case of damage is considered in the code ISO/TS 24817 [10]. To assess the structural integrity of a FRP overwrap repair system, a theoretically based solution is provided to calculate the released energy in case of FRP/steel interface fracture. In this work an independent analytical fracture mechanics model is derived and subsequently compared to the ISO-approach. Further, several numerical investigations of the assumptions and accuracies implemented in the theoretically derived equations are discussed.

2. Theory

Assuming that the adhesion between the steel substrate and the FRP repair is only given by brittle resin and that all work done in inflating the blister is stored as recoverable elastic strain energy, the principles of *Linear Elastic Fracture Mechanics* (LEFM) can be applied to investigate the behaviour of a pressurised blister formation. According to *Griffth's fracture criterion* [11, 12], fracture is only initiated if the energy release rate Γ is greater than or equal to the fracture toughness G_c. In the case of linear elasticity it follows

$$\Gamma = \frac{p\,dV}{2\,dA} \geq G_c \tag{1}$$

where p is the applied pressure, and dV equals the change of blister volume during an infinitesimal crack advance dA [13]. On the basis of Equation (1) two different scenarios can be considered. First, for laboratory testings, the crack resistance G_c can be determined knowing the critical pressure of failure p_{crit} and the material parameters, i.e. the applied repair thickness t and the elastic constants of Young's Modulus E, shear modulus G, and Poisson's ratio ν. The second scenario is the case of application. Knowing, the fracture toughness G_c and the design pressure p, the required material parameter to avoid fracture can be determined by applying an upper limit of the occurring blister volume dV. However, both scenarios have in common that the function of the volume V, with $V(E, G, \nu, t)$, is known. Therefore, an analytical fracture mechanics model is developed in the following.

3. Analytical Analysis of Blister Formation

Provided that the rotation of the cross-section of the repair is zero $r = R$, the behaviour of the pressurised repair is regarded to be equivalent to the one of a clamped circular plate, radius R, under uniform load p, as per Figure 1. Further, it is supposed that the FRP repair can be regarded as a quasi-isotropic laminate, i.e. the in-plane elastic constants are given by $E = E_{11} = E_{22}$ and $\nu = \nu_{12} = \nu_{21}$.
The most significant modes of deformation that contribute to blister volume are assumed to be due to bending $w_b(r)$, transverse shear deformation $w_s(r)$ and local through-thickness compression $w_c'(r)$. The first two modes refer to the r-θ-z coordinate system which lies at the level of the repair mid-surface, as per Figure 1. To consider the additional volumetric deflection due to through-thickness compression, the coordinate system r-θ-z' is introduced, with $z' = z - t/2$, as per Figure 3.
Assuming that the occurring deformations are small, the profile of the bending deflection component $w_b(r)$ for a clamped circular plate of radius R, carrying a uniformly distributed load p, is given after the *Classical Plate Theory* (CPT) [14] by

$$w_b(r) = \frac{p}{64K}(R^2 - r^2)^2 \tag{2}$$

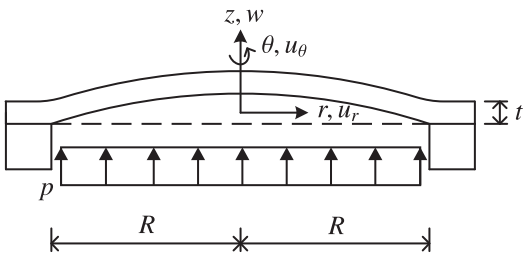

Figure 1: Model of Pressurised Blister

where K, known as flexural rigidity of the plate, is defined as

$$K = \frac{Et^3}{12(1-\nu^2)} \tag{3}$$

In case of the problem given, a high aspect ratio of repair thickness t to hole radius R, and a low transverse shear modulus G ($= G_{13} = G_{23}$) compared to the in-plane shear modulus G_{12}, can result in a large proportion of the total deflection $w(r)$ associated with transverse shear. As the effects of transverse shear strains can often be neglected compared to those involved with bending, the case of a circular transverse elastic plate can be hardly found in literature. Therefore, an approach to determine the quantity of transverse shear deflection $w_s(r)$, based on the ideas of [14, 15] will be derived in detail in the upcoming paragraph.
Considering the kinematics of a transverse elastic plate, as per Figure 2, it can be stated that the total plate rotation $\psi_r(r)$ is given by the strain-displacement relationship

$$\gamma_{rz} = \psi_r + w_{,r} \tag{4}$$

where $[\ldots]_{,r}$ refers to differentiation with respect to radius r and

$$u_r(z) = \psi_r z \tag{5}$$

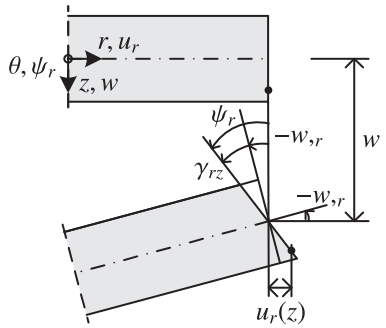

Figure 2: Plate Kinematics

The transverse shear stress τ_{rz}, which has a parabolic distribution over the plate thickness, is given by

$$\tau_{rz}(z) = G\gamma_{rz} = \frac{3}{2t} q_r \left(1 - \frac{4z^2}{t^2}\right) \tag{6}$$

With the use of Equation (5) and Equation (6), the horizontal deflection $u_r(z)$ can be calculated by integrating to

$$u_r(z) = \int \frac{\tau_{rz}(z)}{G} - w_{,r}\, dz = \frac{3}{2Gt} q_r \left(z - \frac{4z^3}{3t^2}\right) - z w_{,r} \tag{7}$$

where the boundary condition $u_r(0) = 0$ was applied. Hence, the strain components ε_r and ε_θ for a rotationally symmetric plate are given by, see e.g. [15]

$$\begin{aligned}\varepsilon_r &= u_{r,r} = \frac{3}{2Gt} q_{r,r} \left(z - \frac{4z^3}{3t^2} \right) - z w_{,rr} \\ \varepsilon_\theta &= \frac{u}{r} = \frac{3}{2Gt} \frac{q_r}{r} \left(z - \frac{4z^3}{3t^2} \right) - \frac{z w_{,r}}{r}\end{aligned} \tag{8}$$

The resulting normal stresses σ_r and σ_θ are generally defined as, see e.g. [15]

$$\begin{aligned}\sigma_r &= \frac{E}{1-\nu^2} (\varepsilon_r + \nu \varepsilon_\theta) \\ \sigma_\theta &= \frac{E}{1-\nu^2} (\nu \varepsilon_r + \varepsilon_\theta)\end{aligned} \tag{9}$$

and thus, the stresses σ_r and σ_θ due to the deflection $u_r(z)$ can be calculated to be

$$\begin{aligned}\sigma_r &= \frac{E}{1-\nu^2} \left(\frac{3}{2Gt} (z - \frac{4z^3}{3t^2}) (q_{r,r} + \nu \frac{q_r}{r}) - z (w_{,rr} + \nu \frac{w_{,r}}{r}) \right) \\ \sigma_\theta &= \frac{E}{1-\nu^2} \left(\frac{3}{2Gt} (z - \frac{4z^3}{3t^2}) (\nu q_{r,r} + \frac{q_r}{r}) - z (\nu w_{,rr} + \frac{w_{,r}}{r}) \right)\end{aligned} \tag{10}$$

Bending moments can be calculated by integrating plate stresses. Thus, the equations for a rotationally symmetric plate are given by

$$\begin{aligned}m_r &= \int_{-t/2}^{t/2} \sigma_r z \, dz \\ &= \frac{E}{1-\nu^2} \left(\frac{t^2}{10G} (q_{r,r} + \nu \frac{q_r}{r}) - \frac{t^3}{12} (w_{,rr} + \nu \frac{w_{,r}}{r}) \right) \\ m_\theta &= \int_{-t/2}^{t/2} \sigma_\theta z \, dz \\ &= \frac{E}{1-\nu^2} \left(\frac{t^2}{10G} (\nu q_{r,r} + \frac{q_r}{r}) - \frac{t^3}{12} (\nu w_{,rr} + \frac{w_{,r}}{r}) \right)\end{aligned} \tag{11}$$

Until this point no differentiation between bending $w_b(r)$ and shear deflection $w_s(r)$ was made. Therefore, the total deflection $w(r)$ is replaced by the sum of $w_b(r) + w_s(r)$ which leads

$$\begin{aligned}m_r =& \frac{E}{1-\nu^2} \left(\frac{t^2}{10G} (q_{r,r} + \nu \frac{q_r}{r}) - \frac{t^3}{12} (w_{s,rr} + \nu \frac{w_{s,r}}{r}) \right) \\ & - K (w_{b,rr} + \nu \frac{w_{b,r}}{r}) \\ m_\theta =& \frac{E}{1-\nu^2} \left(\frac{t^2}{10G} (\nu q_{r,r} + \frac{q_r}{r}) - \frac{t^3}{12} (\nu w_{s,rr} + \frac{w_{s,r}}{r}) \right) \\ & - K (\nu w_{b,rr} + \frac{w_{b,r}}{r})\end{aligned} \tag{12}$$

It is stated that each second part of the above given equations equals the generally accepted expressions for the bending moments $m_{r,b}$ and $m_{\theta,b}$ which can be derived for a transverse rigid plate, i.e. by neglecting the effects of transverse shear strains, see e.g. [14].

$$\begin{aligned}m_{r,b} &= -K (w_{b,rr} + \nu \frac{w_{b,r}}{r}) \\ m_{\theta,b} &= -K (\nu w_{b,rr} + \frac{w_{b,r}}{r})\end{aligned} \tag{13}$$

To assure that the total deflection $w(r)$ can actually be separated into its single components $w_b(r)$ and $w_s(r)$, it is necessary that the bending moments $m_{r,s}$ and $m_{\theta,s}$ due to shear drop out. As a consequence, the deflection $w_b(r)$ only results from bending and $w_s(r)$ from shear forces. It follows

$$\begin{aligned} m_{r,s} &= \frac{E}{1-\nu^2}\left(\frac{t^2}{10G}(q_{r,r}+\nu\frac{q_r}{r}) - \frac{t^3}{12}(w_{s,rr}+\nu\frac{w_{s,r}}{r})\right) \stackrel{!}{=} 0 \\ m_{\theta,s} &= \frac{E}{1-\nu^2}\left(\frac{t^2}{10G}(\nu q_{r,r}+\frac{q_r}{r}) - \frac{t^3}{12}(\nu w_{s,rr}+\frac{w_{s,r}}{r})\right) \stackrel{!}{=} 0 \end{aligned} \tag{14}$$

The arising system of equations can be solved by equating the terms in parentheses which yields

$$w_{s,r}(r) = \frac{6}{5Gt}q_r \tag{15}$$

Applying equilibrium conditions it can be seen that the resultant of the applied load p is equal to the resultant of the reaction forces, which are defined positive in positive z-direction

$$q_r = -\frac{pr}{2} \tag{16}$$

and hence, Equation (15) becomes

$$w_{s,r}(r) = -\frac{3pr}{5Gt} \tag{17}$$

Finally, integrating and applying the edge condition $w_s(R) = 0$ leads to an expression for the shear deflection $w_s(r)$:

$$w_s(r) = \int_0^R w_{s,r}(r)\,dr = \frac{3p}{10Gt}(R^2 - r^2) \tag{18}$$

It is supposed that, in addition to these components there will some further volumetric deflection due to local compression of the repair material under pressure. A first approximation to determine the quantity of this component can be made by comparing the occurring compression to the one around the upper half of a *penny-shaped crack* under internal pressure. This problem was originally considered by Sneddon [16] who calculated the conditions of rupture for an infinite solid containing a plane crack bounded by a circle. It was found that the crack, assumed to be originally an infinitely thin crevice, has, after the application of an internal pressure p, the shape of a very flat ellipsoid of revolution, where the vertical deflection is given by $w_c'(r)$. A schemtical illustration of the undeformed and the deformed crack is shown in Figure 3. It is again noted that the coordinate system r-θ-z' is introduced, with $z' = z - t/2$, to consider the deflection of the bottom edge of the repair.

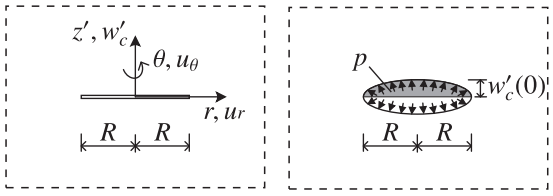

Figure 3: Undeformed and Deformed Penny-Shaped Crack

With the use of equilibrium conditions for an axisymmetric volume element described by cylindrical coordinates, Harding and Sneddon [17] solved the arising system of equations by applying the following boundary conditions on the plane $z' = 0$:

(i) $\tau_{rz'}(r) = 0$ for all values of r
(ii) $\sigma_{z'}(r) = -p(r)$ for $r < R$

(iii) $w_c'(r) = 0$ for $r > R$

Further, due to the rotational symmetry of the problem all derivatives with respect to θ are zero, as well as the stresses $\tau_{r\theta} = \tau_{z'\theta} = 0$. Concerning the remaining stress components $\sigma_r, \sigma_{z'}, \sigma_\theta, \tau_{rz'}$ it is noted that they have to tend to zero as $r \to \infty$ and/or $z' \to \infty$. If it is supposed that the applied pressure $p(r)$ is constant over the entire crack surface $0 \leq r \leq R$, the deflection component $w_c'(r)$ is given by [16, 18]

$$w_c'(r) = \frac{4p(1-\nu_{13}^2)}{\pi E_{33}}(R^2 - r^2)^{0.5} \tag{19}$$

It is obvious that the quantity of this component is determined by the transverse elastic constants E_{33} and ν_{13} to be applied in case of a quasi-isotropic material.
Finally, the volume of fluid in the pressurised blister due to bending (V_b), transverse shear (V_s) and through-thickness compression (V_c) is deduced from the sum of the three deflections by integrating:

$$\begin{aligned} V &= 2\pi \int_{r=0}^{r=R} w(r) r \, dr \\ &= 2\pi \int_{r=0}^{r=R} \left(w_b(r) + w_s(r) + w_c'(r) \right) r \, dr \\ &= \underbrace{\frac{\pi p(1-\nu^2)R^6}{16Et^3}}_{V_b} + \underbrace{\frac{3\pi p R^4}{20Gt}}_{V_s} + \underbrace{\frac{8p(1-\nu_{13}^2)R^3}{3E_{33}}}_{V_c} \end{aligned} \tag{20}$$

For convenience, an illustration of the occurring total blister volumes is given in Figure 4.

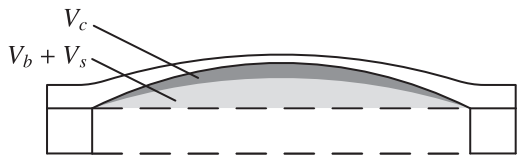

Figure 4: Total Blister Volume

The actual proportion of each volumetric deflection component of the total deflection is illustrated in Figure 5. The calculation is based on representative composite material parameters for a single ply, lamina, as given in Table 1, where the principles of the *Classical Laminate Theory* (CLT) were applied to determine the constants of a quasi-isotropic laminate (Q-I), with $[0°, \pm 60°]_s$ [19]. The other parameter are given by $p = 10\,MPa$, $R = 10\,mm$ and $t = 5\,mm$.
As already introduced above, the energy release rate Γ equals the change of potential energy $-d\Pi$ during an infinitesimally small crack advance dA. In the case to be investigated the area of the crack is given by $A = \pi R^2$ and thus,

$$dA = 2\pi R \, dR \tag{21}$$

Differentiating Equation (20) with respect to R and using Equation (21) to substitute dA leads to an expression for the energy release rate Γ in case of a circular blister formation:

$$\Gamma = p^2 \left[\frac{3(1-\nu^2)}{32Et^3} R^4 + \frac{3}{20Gt} R^2 + \frac{2(1-\nu_{13}^2)}{E_{33}\pi} R \right] \tag{22}$$

With Equation (22) an expression is deduced relating the energy release rate to the pressure, repair geometry and material properties. Substituting radius R by its diameter $d/2$ and Γ by the fracture toughness G_c, as well as considering

Parameter	Lamina	Laminate (Q-I)
$E_{11}\,[GPa]$	30.2	14.8
$E_{22}\,[GPa]$	7.4	14.8
$E_{33}\,[GPa]$	7.4	7.4
$G_{12}\,[GPa]$	2.9	5.7
$G_{13}\,[GPa]$	2.9	2.7
$G_{23}\,[GPa]$	2.6	2.7
$\nu_{12}\,[-]$	0.30	0.31
$\nu_{13}\,[-]$	0.30	0.35
$\nu_{23}\,[-]$	0.42	0.35

Table 1: Repair Material Parameter

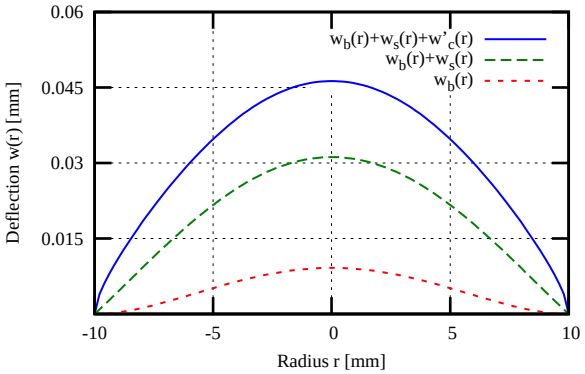

Figure 5: Deflection Curves of Blister

a number of n tests, where $i = 1, 2, \ldots, n$, Equation (22) becomes

$$p_i = \sqrt{\frac{G_{c,i}}{\frac{(1-\nu^2)}{E}\frac{3}{512t_i^3}d_i^4 + \frac{(1-\nu_{13}^2)}{E_{33}}\frac{1}{\pi}d_i + \frac{3}{80Gt_i}d_i^2}} \tag{23}$$

It is stated that under the initially made assumptions Equation (23) is very similar to the corresponding equation which can be found in the ISO-Code [10] as follows

$$p_i = \sqrt{\frac{G_{c,i}}{\frac{(1-\nu^2)}{E_{ac}}\left(\frac{3}{512t_i^3}d_i^4 + \frac{1}{\pi}d_i\right) + \frac{3}{64Gt_i}d_i^2}} \tag{24}$$

However, a detailed comparison of both approaches highlights several differences. First, the ISO-Code uses a combined tensile modulus $E_{ac} = \sqrt{E_{11} \cdot E_{22}}$ to consider a quasi-isotropic material behaviour. This simplification is imprecise and not conform with the principles of the CLT. Further, it can be found that the used expression for transverse shear deflection in the ISO-Code is overestimating the problem. It is supposed that it is based on the erroneous assumption that the shear stress $\tau_{rz}(z)$ has a constant value of $\tau_{rz}(0) = \tau_{max}$ over the plate thickness (cf. Equation (6)). Finally, if a deflection due to through-thickness compression shall be considered it is inevitable to use through-thickness Young's Modulus E_{33} and Poission's ratio ν_{13} for the corresponding compression term. This can yield significantly higher deflections than those obtained when the in-plane constants E_{11} (= E_{22}) and ν_{12} (= ν_{21}) are applied, as found in the ISO-approach. At this point it is generally stated that after Equation (1) an overestimation of volumetric deflection leads to an underestimation of the critical pressure of failure p_{crit} and vice versa.

4. Numerical Analysis of Blister Formation

The analytical fracture mechanics model of a pressurised blister represents a first method to calculate the released energy in case of steel/FRP-interface fracture. In order to assess the assumptions made in this approach, several numerical investigations based on *Finite Element Analysis* (FEA) are conducted. As discussed above the total volumetric deflection can be separated in three different modes – bending, transverse shear and through-thickness compression. To prove the accuracy of each analytically derived term, a similar model geometry is required. Therefore, a clamped circular plate with radius $R = 10\,mm$, thickness $t = 2.5\,mm$ ($t = 5.0\,mm$) and load $p = 10\,MPa$ is modeled. The applied material properties are the same as the ones of the quasi-isotropic laminate, as introduced in Table 1. Due to the rotational symmetry of the entire problem, including material properties, orthotropic axisymmetric nine-node solid elements are used [20]. To ensure that the occurring deformations are computed sufficiently precise, a number of 10 elements are used in through-thickness z-direction (20 elements for $t = 5.0\,mm$). In radial r-direction the number of elements is 40. It is noted that due to symmetry conditions an equivalent modeling strategy could be the implementation of a three-dimensional segment of a circle with an arbitrary opening angle.
In terms of cylindrical coordinates, the indices 1, 2, 3 are replaced by r, θ, z. Accordingly, the stress-strain relations of an orthotropic axisymmetric solid element are given by, see e.g. [15]

$$\begin{bmatrix} \varepsilon_r \\ \varepsilon_\theta \\ \gamma_{rz} \\ \varepsilon_z \end{bmatrix} = \begin{bmatrix} \frac{1}{E_{rr}} & -\frac{\nu_{r\theta}}{E_{rr}} & 0 & -\frac{\nu_{rz}}{E_{rr}} \\ & \frac{1}{E_{\theta\theta}} & 0 & -\frac{\nu_{\theta z}}{E_{\theta\theta}} \\ sym. & & \frac{1}{G_{rz}} & 0 \\ & & & \frac{1}{E_{zz}} \end{bmatrix} \begin{bmatrix} \sigma_r \\ \sigma_\theta \\ \tau_{rz} \\ \sigma_z \end{bmatrix} \tag{25}$$

As it can be seen from Equation (25) shear strains are generally not coupled to extensional loading in case of an orthotropic material. Hence, it is supposed that the portion of bending deflection $w_b(r)$ of the overall deflection $w(r)$ can be extracted by a high increase of the transverse shear stiffness G_{rz} (used factor = 100). To exclude additional deflection due to a compression and/or contraction of the plate, the load is divided in one half each on the bottom and the upper edge of the plate, and the deflection is analysed at the level of the mid-surface. The analytical term for bending deflection $w_b(r)$ and the deflection curve achieved by FEA are illustrated in Figure 6 for both plate geometries. It can be seen that the curves show a high concordance.

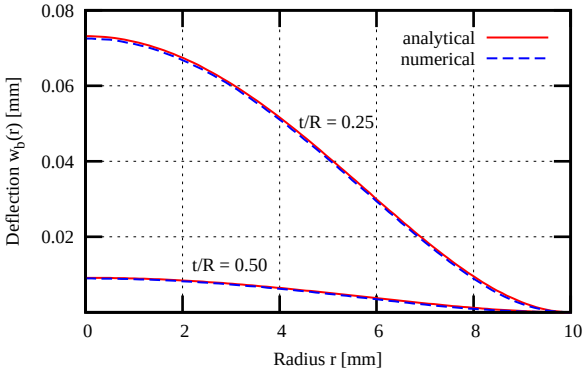

Figure 6: Bending Deflection ($R = 10\,mm$)

Since the CPT, which is basis for the analytical derivation of $w_b(r)$, basically requires a small ratio of t/R, it is obvious that the accuracy of the analytical approach declines with increasing ratio of t/R. To this effect, it could be shown that an adequate accuracy is only obtained for $t/R \leq 0.5$, otherwise this component is overestimated.

As an extraction of pure shear deflection is not possible, the total deflection due to bending and shear is investigated. Applying the same model as before, but using the actual non-modified material properties (cf. Table 1), it is found that the analytical and the numerical approach also yield similar deflection curves, as per Figure 7. Therefore, it is stated that the analytically derived term for transverse shear deflection $w_s(r)$ works accurately as well for $t/R \leq 0.5$.

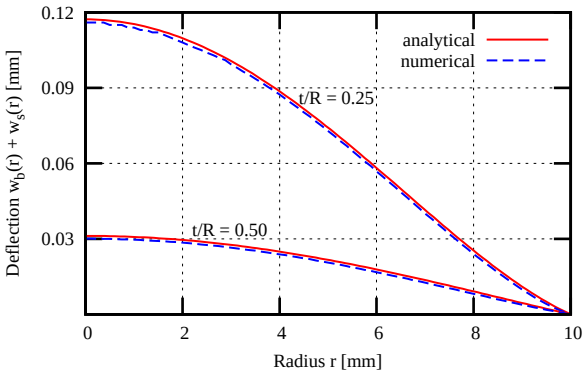

Figure 7: Bending and Transverse Shear Deflection ($R = 10\,mm$)

In order to investigate the effect of an additional volumetric deflection due to through-thickness compression, the load p is fully applied on the bottom edge of the plate. Provided that neither bending nor shear deflection vary over the plate thickness, the quantity of compression can be estimated by calculating the difference in deflection of the bottom edge and the mid-surface. To this effect, it is found that the percentage increase in deformation at $r = 0$ is vanishingly small for $t = 5\,mm$ ($t/R = 0.5$), but already amounts to 39% for $t = 10\,mm$ ($t/R = 1.0$), indicating that the influence of compression increases with increasing ratio t/R. Accordingly, Figure 8 shows a comparison between the calculated deflection curves due to through-thickness compression obtained by FEA and the analytical solution $w_c'(r)$ after [16].

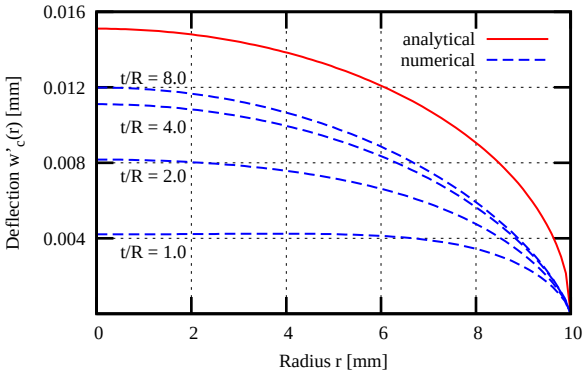

Figure 8: Convergence Study of Through-Thickness Compression

Evidently, the numerical results converge to a final deflection with increasing ratio t/R. Although, it is found that even for a solid with $t/R = 8$, this deflection is still lower than $w_c'(r)$. The reason for this difference in deformation can be found in the origin of $w_c'(r)$. Sneddon [16] investigated the extension of a penny-shaped crack in an infinite solid, stressed with an internal pressure. Consequently, the occurring deformations are not affected by any constraints and the possible influence of a varying thickness t is not considered in the final deflection term, as per Equation (19).
Nevertheless, to demonstrate the effectivity of $w_c'(r)$ for an infinite solid, the same axisymmetric structure and procedure are applied as introduced above, however, to exclude any constraints due to boundary conditions not only a high thickness of $t = 80\,mm$ is applied, but the radial dimension of the solid is also extended to $20\,mm$. Further, only one

half of the bottom edge is pressurised, where the other half is fixed in through-thickness z-direction. The structure is illustrated in Figure 9 showing the vertical displacement in a contour-plot.

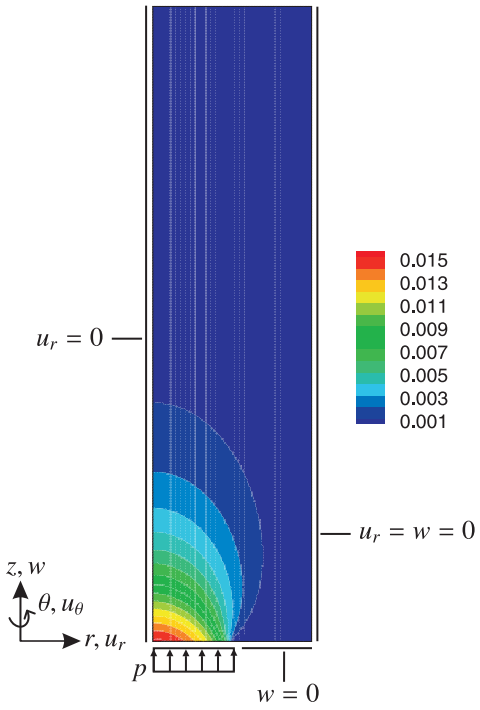

Figure 9: FEA of Penny-shaped Crack Model: System, Loading, Boundary Conditions and Distribution of $w(r)$

In this case both approaches yield identical deflection curves, as per Figure 10.
The outcome of this is that a consideration of through-thickness compression in terms of [16] can only be used as a first approximation, provided the applied repair thickness is sufficiently thick. Otherwise the portion of this component is significantly overestimated within the analytical model.

5. Conclusion

The analytical and numerical investigation of a pressurised blister formation has highlighted several inaccuracies implemented in the ISO-Code [10]. Hence, a parabolic distribution of the transverse shear stress τ_{rz} is disregarded in the code's approach which leads to an overestimation of transverse shear effects. Although, it is a conservative assumption it is contradictory to an economic design of the FRP repair.
Further, by the incorrect use of in-plane elastic constants, the theoretical effects of through-thickness compression can be underestimated. As above-mentioned, an underestimation of blister volume leads to an overestimation of the critical pressure p_{crit} and is thus not acceptable.
A comparison of the analytical and the numerical model has shown that the theoretically derived deflection terms for bending and transverse shear work accurately, provided a sufficiently small ratio of plate thickness t to plate radius R. On the contrary, it is found that a consideration of through-thickness compression is only justifiable for $t/R > 0.5$, i.e. when the effects of bending and shear deformation can be neglected due to the compact geometry of the structure.
Further, it is stated that even for thick repairs the application of the approach after [16] can only be used as a first approximation. Hence, it is recommended to introduce a reduction factor considering decreasing compression due to decreasing thickness.
Finally, it still needs to be clarified whether the idea of reducing the problem to the one of a clamped circular plate is possibly underestimating the problem, i.e. the volume of the blister. According to this, it is expected that especially

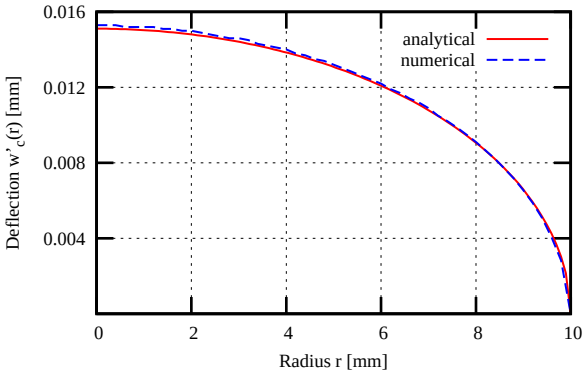

Figure 10: Deflection of Penny-Shaped Crack Model

in case of thin repairs the compliance of the surrounding repair material, with $r > R$, leads to a higher volumetric deflection. Due to the high complexity in deducing an analytical approach for a plate based on a compliant support, several FEA of different models have to be investigated to assess these effects and to determine possible increase factors.

Acknowledgments

This work was performed within the project *Structure Repair and Rehabilitation* of the Cooperative Research Centre for Advanced Composite Structures (CRC-ACS) Ltd in Melbourne, Australia. The lead author would like to acknowledge and thank CRC-ACS, particularly Professor Murray Scott and David Elder, for their invaluable assistance, support and guidance throughout this research. The author is also grateful for the financial support provided by the German Academic Exchange Service (DAAD).

References

[1] Batisse R. Review of gas transmission pipeline repair methods. In: Safety, Reliability and Risks Associated with Water, Oil and Gas Pipelines. NATO Science for Peace and Security Series C: Environmental Security; Springer Netherlands; 2008, p. 335–49.
[2] Baker A. Bonded composite repair of fatigue-cracked primary aircraft structure. Composite Structures 1999;47:431–43.
[3] Tavakkolizadeh M, Saadatmanesh H. Strengthening of steel-concrete composite girders using carbon fiber reinforced polymers sheets. Journal of Structural Engineering 2003;129:30–40.
[4] Buyukozturk O, Hearing B. Failure behavior of precracked concrete beams retrofitted with FRP. Journal of Composites for Construction 1998;2:134–44.
[5] Duell JM, Wilson JM, Kessler MR. Analysis of a carbon composite overwrap pipeline repair system. International Journal of Pressure Vessels and Piping 2008;85:782–8.
[6] Goertzen WK, Kessler MR. Dynamic mechanical analysis of carbon/epoxy composites for structural pipeline repair. Composites Part B: Engineering 2007;38:1–9.
[7] Wagner W, Balzani C. Simulation of delamination in stringer stiffened fiber-reinforced composite shells. Computers & Structures 2008;86:930–9.
[8] Balzani C, Wagner W. An interface element for the simulation of delamination in unidirectional fiber-reinforced composite laminates. Engineering Fracture Mechanics 2008;75:2597–615.
[9] Mableson AR, Dunn KR, Dodds N, Gibson AG. Refurbishment of steel tubular pipes using composite materials. Plastics, Rubber and Composites 2000;29:558–65.
[10] ISO/TS 24817:2006: Petroleum, petrochemical and natural gas industries - composite repairs for pipework - qualification and design, installation, testing and inspection. Standard; International Organization for Standardization, Geneva, Switzerland; 2006.
[11] Griffith AA. The phenomena of rupture and flow in solids. Philosophical Transactions of the Royal Society of London 1921;221:163–98.
[12] Wang CH. Introduction to fracture mechanics. General document DSTO-GD-0103; Defence Sience and Technology Organisation; 1996.
[13] Gross D, Seelig T. Linear fracture mechanics. In: Fracture Mechanics. Mechanical Engineering Series; Springer Berlin Heidelberg; 2011, p. 63–144.
[14] Timoshenko S, Woinowsky-Krieger S. Theory of plates and shells. Engineering Societies Monographs; McGraw-Hill; 1959.
[15] Panc V. Theories of elastic plates. Mechanics of Surface Structures Series; Noordhoff International Pub.; 1975.

[16] Sneddon IN. The distribution of stress in the neighbourhood of a crack in an elastic solid. Proceedings of the Royal Society of London Series A Mathematical and Physical Sciences 1946;187:229–60.
[17] Harding JW, Sneddon IN. The elastic stresses produced by the indentation of the plane surface of a semi-infinite elastic solid by a rigid punch. Mathematical Proceedings of the Cambridge Philosophical Society 1945;41:16–26.
[18] Key PL. A relation between crack surface displacements and the strain energy release rate. International Journal of Fracture 1969;5:287–96.
[19] Gibson RF. Principles of composite material mechanics. Mechanical Engineering Series; CRC Press; 2. ed.; 2007.
[20] Taylor RL. FEAP – a finite element analysis program. Theory manual version 8.3; Department of Civil and Environmental Engineering, University of California at Berkeley; 2011. URL `www.ce.berkeley.edu/projects/feap/theory.pdf`.